

몬테카를로 방사선해석 (Monte Carlo Radiation Analysis)

Electron Transport Modeling

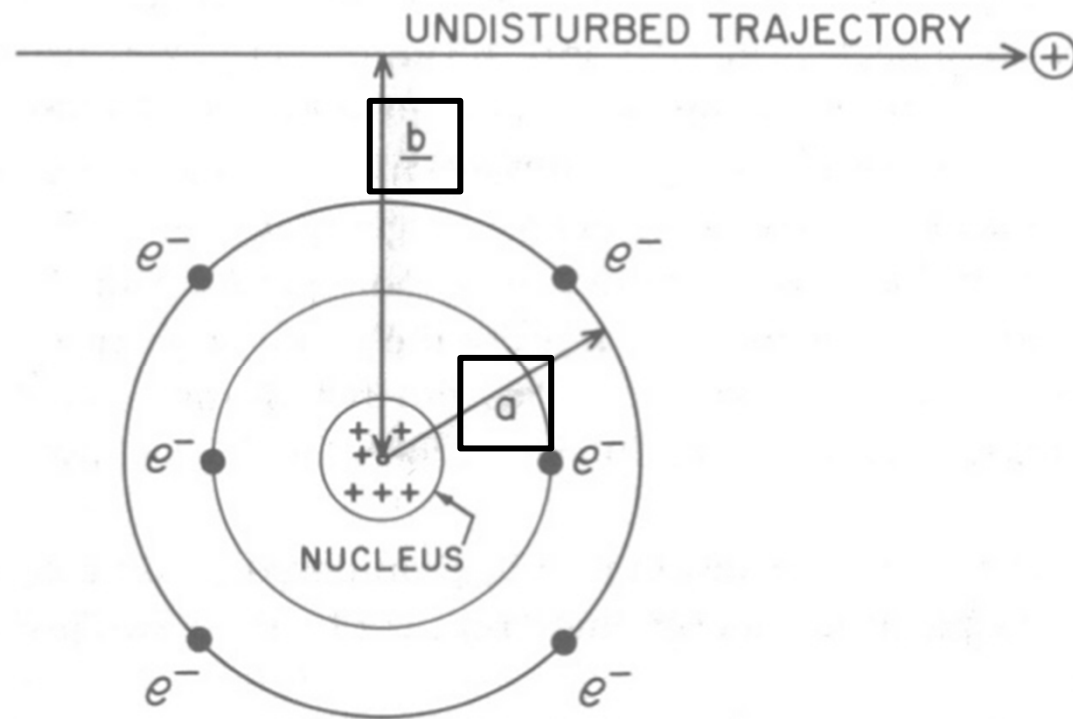
Notice: This document is prepared and distributed for educational purposes only.

Review on Charged Particle Interactions

✓ Charged Particles: energy transfer mechanism

- Ionization/Excitation
 - kinetic energy of the ejected electron
= energy loss - ionization potential
 - delta ray: the ejected electron of kinetic energy high enough to cause ionizations itself
- bremsstrahlung
 - x-rays emitted when high-speed charged particles accelerate near the nucleus
 - likelihood increasing with atomic number of the medium
 - continuous energy spectrum with an endpoint energy equal to the particle kinetic energy

✓ Charged particles' trajectories



atomic radius (a) vs. impact parameter (the shortest distance) (b) in charged particle trajectory

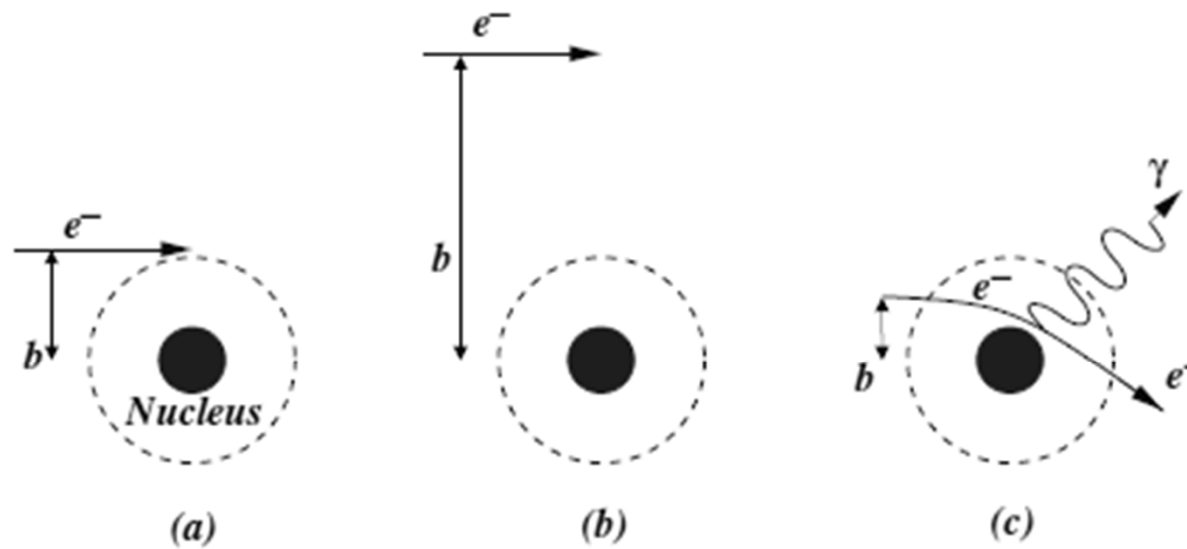


Figure 2.4: Collision types in the Coulomb interaction: (a) Hard collision, in which the impact parameter b is of the order of the atomic radius, (b) Soft collision, in which $b \gg a$, and (c) Radiation collision, where $b \ll a$.

(source: John Kildea, Master Thesis, 2010)

✓ Charged particles: collisional energy loss

- Soft collision ($b \gg a$)
 - When a charged particle passes an atom at a considerable distance, the charged particle's Coulomb force affects the atom as a whole, thereby distorting, exciting or ionizing the atom.
 - The net effect is the transfer of a very small amount of energy to an atom of the medium.
 - the most probable type of interaction at large b values → accounts for roughly half of the energy transfer to the absorbing medium.
 - In condensed media (liquids and solids), the atomic distortion gives rise to the density effect.
 - Under certain conditions, a very small part of the energy spent in soft collision can be emitted by the medium as bluish-white light called Cerenkov radiation (vs. bremsstrahlung near nucleus).

✓ Charged particles: collisional energy loss (cont.)

- Hard collision ($b \sim a$)
 - When a charged particle passes an atom at a distance of the order of atomic dimension, it interacts primarily with a single atomic electron, which is then ejected from the atom with considerable kinetic energy ($\gg E_B$, negligible) (delta-ray).
 - Few in number, but comparable energy loss with that by soft collisions.
 - Whenever inner electron is ejected, characteristic x-ray or Auger electron ejection follows.

$$\frac{Q_{max}}{E_{in}} = \frac{E_{in} - E_{out,min}}{E_{in}} = \frac{4mM}{(M + m)^2}$$

✓ Charged particles: collisional energy loss (cont.)

- Coulomb force interactions with the external nuclear field ($b \ll a$): electrons
 - In 97~98% of interactions,
 - (1) an electron is scattered elastically and does not emit an x-ray photon or excite the nucleus;
 - (2) it loses an insignificant amount of energy necessary to satisfy conservation of momentum for the collision;
 - (3) an important means of deflecting electrons, which explains
 - why electrons follow tortuous paths, especially in high-Z media and why electron backscattering increases with Z;
 - (4) the differential elastic scattering cross section per atom is proportional to Z^2 .

✓ Charged particles: collisional energy loss (cont.)

- Coulomb force interactions with the external nuclear field ($b \ll a$): electrons
 - In 2~3% of interactions,
 - (1) an inelastic radiative interaction occurs, in which x-ray photon is emitted (bremsstrahlung);
 - (2) the electron is not only deflected but also gives a significant fraction (up to 100%) of its kinetic energy to the photon.
 - (3) The differential atomic cross section is proportional to Z^2 and also depends on the inverse square of the mass of the charged particle
- Bremsstrahlung generation by charged particles other than electrons is totally insignificant.

✓ Charged particles: collisional energy loss (cont.)

- Coulomb force interactions with the external nuclear field ($b \ll a$): positrons
 - **antimatter (in-flight) annihilation**
 - (1) the remaining kinetic energy of the positron is given to one or both of the annihilation photons.
 - (2) the average fraction of a positron's kinetic energy that is spent in annihilation is comparable to that in bremsstrahlung.

✓ Charged particles: collisional energy loss (cont.)

- Coulomb force interactions with the external nuclear field ($b \ll a$): heavy charged particles with very high energy
 - Heavy charged particles with sufficiently high (~ 100 MeV) energy may interact inelastically with the nucleus
 - When one or more individual nucleons are struck, they are driven out of the nucleus in an "intranuclear cascade" process, collimated strongly in the forward direction.
 - The highly excited nucleus decays by emitting "evaporation particles" (mostly nucleons of relatively low energy) and γ -rays, which are carried away.

✓ Charged Particles: energy loss indices (1)

- Stopping power, S
 - = the energy absorption power of the medium
 - ≡ the expectation value of the energy loss per unit path length

$$S = \frac{dT}{dx} = \left. \frac{dT}{dx} \right|_c + \left. \frac{dT}{dx} \right|_r$$

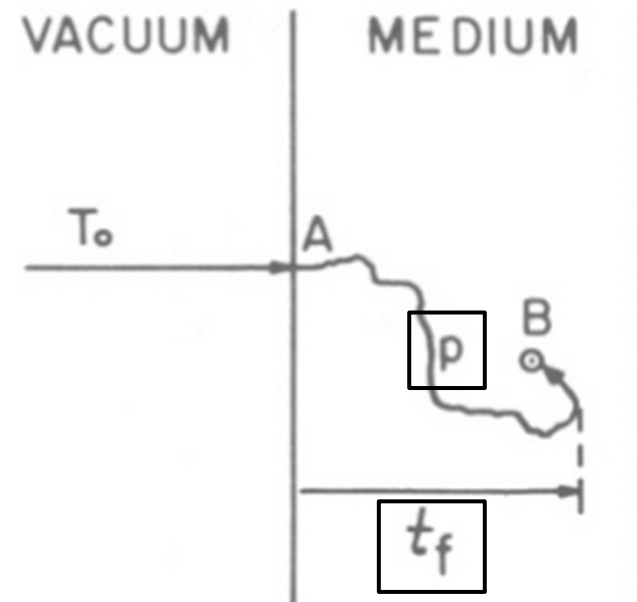
dT = the kinetic energy loss of a charged particle through collisional (c) or radiative (r) interactions while traversing dx

- Mass stopping power, S_ρ

$$S_\rho = \frac{dT}{\rho dx} = \left. \frac{dT}{\rho dx} \right|_c + \left. \frac{dT}{\rho dx} \right|_r$$

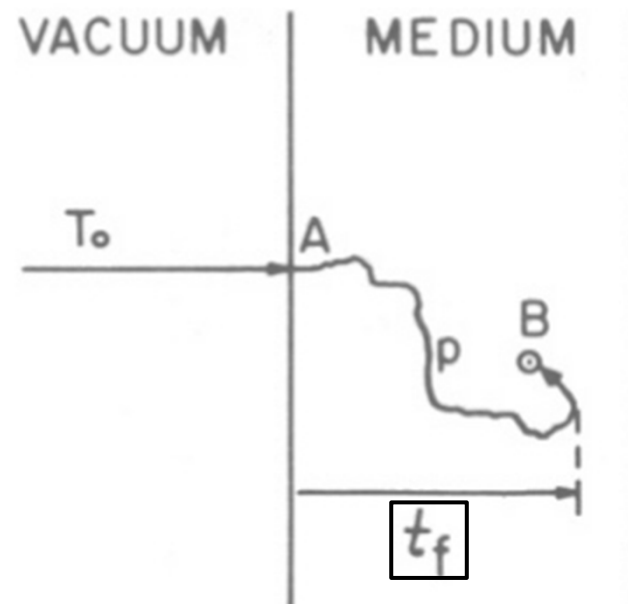
✓ Charged Particles: range (1)

- pathlength, p = the total distance along the path from the point of entry A to the stopping point B .
- "range" R = the expectation value of the pathlength p that the charged particle follows.



✓ Charged Particles: range (2)

- projected range $\langle t_f \rangle$ = the expected value of the farthest depth of penetration t_f of the particle in its initial direction
- t_f is not necessarily the depth of the terminal point



✓ Charged Particles: range (3)

- continuous slowing down approximation (CSDA) range, R_{CSDA}

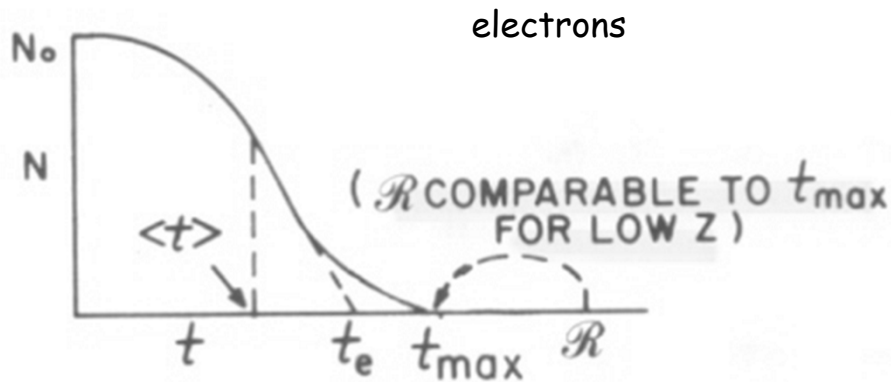
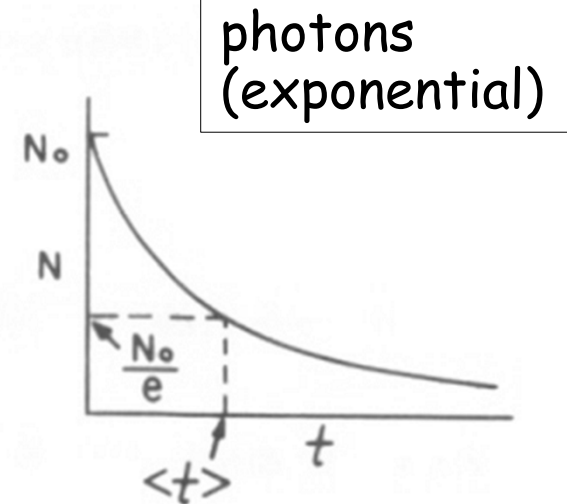
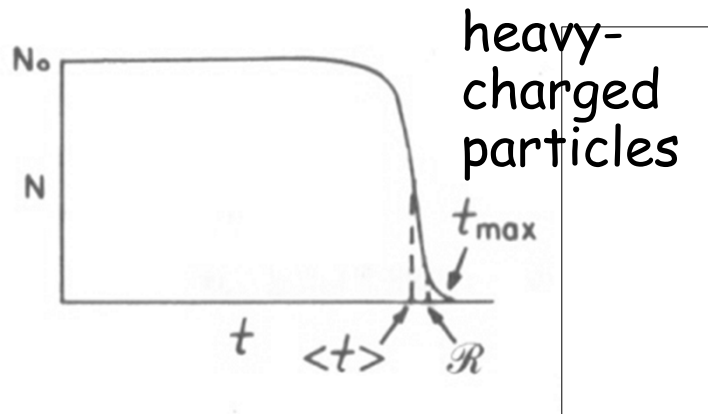
$$R_{\text{CSDA}} = \int_0^{T_0} \left(\frac{dT}{dx} \right)^{-1} dT \quad [\mu\text{m}]$$

- Range is inversely proportional to the density of the absorbing material.
- Mass ranges in different elements

$$\rho_m R_m \propto \rho_{\text{air}} R_{\text{air}} \quad [\text{g} / \mu\text{m}^2]$$

$$\text{where } \rho_m R_m = \int_0^{T_0} \left(\frac{dT}{\rho_m dx} \right)^{-1} dT \quad [\text{g} / \mu\text{m}^2]$$

✓ Radiation Penetration



- extrapolated penetration depth, t_e
= the absorber thickness corresponding to the intersection b/w the extrapolation of the linearly descending portion and the tail of the curve

*Little deflection (multiple scattering) in low-Z matter

Electron Transport

Ion-Atom Scattering

- ✓ *Elastic scattering by electrons of the target atom*
- ✓ *Inelastic scattering by electrons of the target atom*
- ✓ *Elastic scattering by the nucleus of the target atom*
- ✓ *Inelastic scattering by the nucleus of the target atom*

Electron Interactions

➤ Catastrophic events

- hard collision (large energy-loss) Möller scattering ($e^-e^- \rightarrow e^-e^-$): δ -ray emission
- hard collision (large energy-loss) Bhabha scattering ($e^+e^- \rightarrow e^+e^-$): δ -ray emission
- hard bremsstrahlung emission ($e^\pm N \rightarrow e^\pm \gamma N$), and
- positron annihilation “in-flight” and at rest ($e^+e^- \rightarrow \gamma\gamma$).

Electron Interactions (cont.)

➤ *Soft events*

- *low-energy Møller (Bhabha) scattering, (modeled as part of the collision stopping power),*
- *atomic excitation ($e^\pm A \rightarrow e^\pm A^*$) via soft collision (modeled as another part of the collision stopping power),*
- *soft bremsstrahlung (modeled as radiative stopping power), and*
- *elastic electron (positron) multiple scattering from atoms, ($e^\pm N \rightarrow e^\pm N$).*

Hard Bremsstrahlung Production

- ✓ $(e^{\pm}N \rightarrow e^{\pm}\gamma N)$,
- ✓ Bremsstrahlung production is the creation of photons by electrons (or positrons) in the field of an atom.
- ✓ There are two possibilities. The predominant mode is the interaction with the atomic nucleus. This effect dominates by a factor of about Z over the three-body case where an atomic electron recoils. (nucleus $B \propto Z^2$ vs. electron $B \propto Z$)
- ✓ The acceleration/deceleration of an electron scattering from nuclei can be quite violent, resulting in emission of energy of up to the total kinetic energy of the incoming charged particle.

Hard Bremsstrahlung Production (cont.)

- ✓ The nucleus effect ($e^\pm N \rightarrow e^\pm \gamma N$) can be taken into account through the total cross section and angular distribution kinematics.
- ✓ The nucleus effect can be modeled using one of the Koch and Motz formulae (Reviews of Modern Physics, Vol 31, 920, 1959).
- ✓ The bremsstrahlung cross section scales with $Z(Z + \xi(Z))$, where $\xi(Z)$ is the factor accounting for the effect of atomic electrons. These factors can be taken from the work of Tsai. (Reviews of Modern Physics, Vol 49, 421, 1974).
- ✓ The total cross section depends approximately like $1/E_\gamma$.

Bremsstrahlung Cross-Section Formulas and Related Data*

H. W. KOCH AND J. W. MOTZ

National Bureau of Standards, Washington, D. C.

I. Introduction.....	920	IV. Thick-Target Bremsstrahlung Production....	949
II. Bremsstrahlung Cross Sections.....	921	A. Thick-Target Bremsstrahlung Angular Distributions.....	949
A. Symbols, Constants, and Energy-Momentum Relations.....	921	(1) Nonrelativistic and Intermediate Energies.....	949
B. Types of Cross-Section Calculations...	921	(2) Relativistic Energies.....	950
C. Bremsstrahlung Cross-Section Formulas and Classification Diagrams.....	922	B. Thick-Target Bremsstrahlung Spectra..	951
(1) Born-Approximation Cross-Section Formulas.....	926	(1) Nonrelativistic and Intermediate Energies.....	951
(2) Extreme-Relativistic Cross-Section Formulas with the Coulomb Correction.....	927	(2) Relativistic Energies.....	952
D. Graphical Representation of the Formulas.....	927	C. Efficiency for Bremsstrahlung Production.....	953
(1) Dependence of the Bremsstrahlung Spectrum on Electron Energy.....	929	(1) Nonrelativistic and Intermediate Energies.....	955
(2) Dependence of the Bremsstrahlung Spectrum on Photon Angle	929	(2) Relativistic Energies.....	955
(3) Screening Effects and Coulomb Corrections.....	931	(a) Intermediate thickness targets.....	955
E. Corrections for the Cross-Section Formulas.....	931	(b) Thick targets.....	955
(1) Coulomb Corrections.....	931	V. Acknowledgments.....	955
(a) Nonrelativistic energies...	931		

I. INTRODUCTION

CONSIDERABLE information about the bremsstrahlung process has accumulated during the past several years. This information includes various cross-section calculations and measurements, which

Pair production and bremsstrahlung of charged leptons*

Yung-Su Tsai

Stanford Linear Accelerator Centers, Stanford University, Stanford California 94305

Photo pair productions of electrons, muons, and heavy leptons and bremsstrahlung of electrons and muons are reviewed. Atomic and nuclear form factors necessary for these calculations are discussed. Straggling of electrons in matter and other effects due to finite target thickness are considered. Tables of radiation lengths of all materials and the energy dependence of photon absorption coefficients of many materials are presented. Problems associated with production of particles by photon and electron beams are also discussed.

CONTENTS

I. Introduction	815
II. Pair Production Cross Section by Born Approximation	817
III. Approximate Expressions	819
A. Electron pair production	819
1. Arbitrary form factors	820
2. Hydrogen and helium atoms	821
3. Checking the accuracy of Bethe's approximations	823
4. Thomas-Fermi atoms	823
5. Total pair production cross section	826
B. Radiation length of materials	827
C. Muon pair production	829
D. Energy angle distribution of bremsstrahlung	830
E. Bremsstrahlung in colliding beam experiment	831
F. $e^+ + e^- \rightarrow 2\gamma, 3\gamma$	831
G. Muon bremsstrahlung	832
IV. Effects Due to Finite Target Thickness	832

produced by the electron. Hence one has to know accurately the properties of the bremsstrahlung beam in a fairly thick target. The pair production is related to the bremsstrahlung problem by a substitution rule. Thus calculation of the electron pair production cross section is trivial once we know how to calculate the bremsstrahlung by electrons. Muon and heavy-lepton pair productions were also estimated at that time. For production near the forward angle, the electron pair production involves only the atomic form factors, whereas in the muon and heavy-lepton productions, nuclear form factors must be taken into consideration. As the laboratory began to operate and experiments became more precise, many of these calculations also became more refined and efficient. For example, in order to make precise measurements in the photoproduction experiments it is

Reviews of Modern Physics, 49, 421 (1974)

BREMSSTRAHLUNG SPECTRA FROM ELECTRON INTERACTIONS WITH SCREENED ATOMIC NUCLEI AND ORBITAL ELECTRONS *

Stephen M. SELTZER and Martin J. BERGER

*National Bureau of Standards **, Gaithersburg, MD 20899, USA*

Received 6 December 1984 and in revised form 11 February 1985

Through the synthesis of various theoretical results, a comprehensive set of bremsstrahlung cross sections (differential in the energy of the emitted photons) has been prepared. The set includes results for electrons with energies from 1 keV to 10 GeV incident on neutral atoms with atomic numbers $Z = 1$ to 100. For bremsstrahlung in the Coulomb field of the atomic nucleus, use was made of (a) results of Pratt, Tseng, and collaborators based on numerical phase-shift calculations for the screened Coulomb potential at energies below 2 MeV, and (b) the analytical high-energy theory (with Coulomb corrections) of Davies, Bethe, Maximon and Olsen at energies above 50 MeV, supplemented by the Elwert Coulomb correction factor and the theory of the high-frequency limit given by Jabbur and Pratt. In the high-energy region, the effect of screening was included with use of Hartree–Fock atomic form factors. A numerical interpolation scheme, applied to suitably scaled cross sections, was used to bridge the gap between the low-energy and high-energy theoretical results, and thus to obtain improved cross sections in the intermediate-energy region 2 to 50 MeV. Bremsstrahlung in the field of the atomic electrons was calculated according to the theory of Haug, combined with screening corrections derived from Hartree–Fock incoherent scattering factors. The paper also contains numerous comparisons between calculated and measured bremsstrahlung spectra, which indicate generally good agreement.

1. Introduction

Many theories of the bremsstrahlung process have been developed, each with its own approximations, limitations and regions of applicability. To obtain accurate

following: (a) the Born-approximation theory of Bethe and Heitler [1,2] and others [3–7], with inclusion of a form-factor screening correction; (b) the Elwert [8] Coulomb correction factor, derived from Sommerfeld's [9] non-relativistic theory for an unscreened Coulomb

Hard Bremsstrahlung Production (cont.)

- ✓ The cross section can be written as the sum of two terms

$$\boxed{\frac{d\sigma}{dk}} = \frac{d\sigma_n}{dk} + Z \frac{d\sigma_e}{dk}$$

where $d\sigma_n/dk$ represents the bremsstrahlung of energy k in m_0c^2 unit produced in the field of the screened atomic nucleus, and $Z(d\sigma_e/dk)$ represents the bremsstrahlung produced in the field of the Z atomic electrons.

- ✓ It can be rewritten as $\frac{d\sigma}{dk} = \left(1 + \frac{\eta}{Z}\right) \frac{d\sigma_n}{dk}$,

where η is the cross-section ratio $\eta = \frac{d\sigma_e}{dk} / \left(\frac{1}{Z^2} \frac{d\sigma_n}{dk}\right)$

Z^2 -dependency vs. Z -dependency

Hard Bremsstrahlung Production (cont.)

- ✓ The radiation integral for electron of energy E_0 is

$$\phi_{\text{rad}} \equiv \frac{1}{E_0} \int_0^{k_{\text{max}}} k \frac{d\sigma_{\text{Brem}}}{dk} dk : \text{Heitler}$$

(Heitler W. "The Quantum Theory of Radiation", Oxford Univ. Press. 154)

- ✓ The Koch and Motz formulae for electron-nucleus interaction by Born approximation are

$$d\sigma_k = \frac{4Z^2 r_0^2 dk}{137 k} \left\{ \left[1 + \left(\frac{E}{E_0} \right)^2 - \frac{2E}{3E_0} \right] \ln(183Z^{-1}) + \frac{1}{9} \frac{E}{E_0} \right\}$$

and

$$\phi_{\text{rad}} = \frac{4Z^2 r_0^2}{137} \left[\ln(183Z^{-1}) + \frac{1}{18} \right]$$

in completely screened nuclear field, where $r_0 =$ classical electron radius and $\alpha =$ the fine structure constant.

Ex. Formulae of Koch and Motz (1959)

Formula 1BS—Differential in photon energy and in photon and electron emission angles. *for high E_0 and E ($\gg E_B$)*
 Approximation (H). Reference formulas: (13) in reference (a), (2) in reference (b), (13) in reference (c), (29) in reference (e).

$$d\sigma_{k,\theta_0,\theta,\phi} = \frac{Z^2}{137} \left(\frac{r_0}{2\pi} \right)^2 [1 - F(q,Z)]^2 \frac{dk}{k} \frac{p}{p_0} \frac{d\Omega_k d\Omega_p}{q^4} \left\{ \frac{p^2 \sin^2\theta}{(E - p \cos\theta)^2} (4E_0^2 - q^2) + \frac{p_0^2 \sin^2\theta_0}{(E_0 - p_0 \cos\theta_0)^2} (4E^2 - q^2) \right. \\ \left. - \frac{2pp_0 \sin\theta \sin\theta_0 \cos\phi (4EE_0 - q^2)}{(E - p \cos\theta)(E_0 - p_0 \cos\theta_0)} + \frac{2k^2(p^2 \sin^2\theta + p_0^2 \sin^2\theta_0 - 2pp_0 \sin\theta \sin\theta_0 \cos\phi)}{(E - p \cos\theta)(E_0 - p_0 \cos\theta_0)} \right\},$$

where

$$q^2 = p^2 + p_0^2 + k^2 - 2p_0k \cos\theta_0 + 2pk \cos\theta - 2p_0p(\cos\theta \cos\theta_0 + \sin\theta \sin\theta_0 \cos\phi)$$

and $F(q,z)$ = atomic form factor discussed in Sec. IIE(3).

Formula 2BN(a)—Differential in photon energy and angle. *by high-energy, small-angle approximation*
 Approximations (H), (B), (J), (K).

$$d\sigma_{k,\theta_0,\phi} = \frac{2Z^2 r_0^2 E}{\pi 137 E_0 k} \frac{dk}{k} d\Omega_k \left\{ \frac{16(\theta_0 E_0)^2 E_0^2}{(1 + \theta_0^2 E_0^2)^4} - \frac{(E_0 + E)^2 E_0}{E(1 + \theta_0^2 E_0^2)^2} + 2 \ln\left(\frac{EE_0}{k}\right) \left[\frac{(E^2 + E_0^2) E_0}{E(1 + \theta_0^2 E_0^2)^2} - \frac{4\theta_0^2 E_0^4}{(1 + \theta_0^2 E_0^2)^4} \right] \right\}.$$

Formula 3BS(a)—Complete screening ($\gamma=0$ or $\phi_1(\gamma=0) = 4 \ln 183$; $\phi_2(\gamma=0) = \phi_1(\gamma=0) - \frac{2}{3}$).
 Formula 3BS with $\gamma=0$.

$$d\sigma_k = \frac{4Z^2 r_0^2 dk}{137 k} \left\{ \left[1 + \left(\frac{E}{E_0} \right)^2 - \frac{2E}{3E_0} \right] \ln(183Z^{-1}) + \frac{1}{9} \frac{E}{E_0} \right\}.$$

Formula 4BS—Total radiation cross section.
 Approximations (H), (F), (J). Reference formulas: (47) in reference (a), (34) in reference (c), (62) in reference (j).

$$\phi_{\text{rad}} = \frac{4Z^2 r_0^2}{137} \left[\ln(183Z^{-1}) + \frac{1}{18} \right].$$

Cross sections $d\sigma_k/dk$ for bremsstrahlung of energy k (from Koch and Motz)

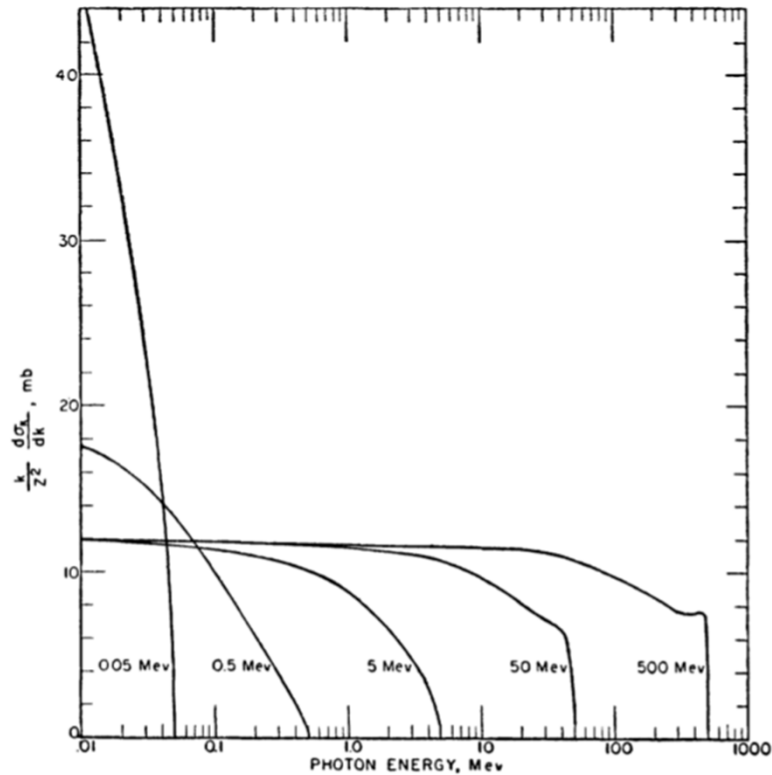


FIG. 3. Dependence of the Born-approximation cross section integrated over the photon directions on the photon and electron energy. The ordinate values for these curves are obtained from Formula 3BN for 0.05- and 0.50-Mev electrons, and from Formula 3BS (e) for 5-, 50-, and 500-Mev electrons.

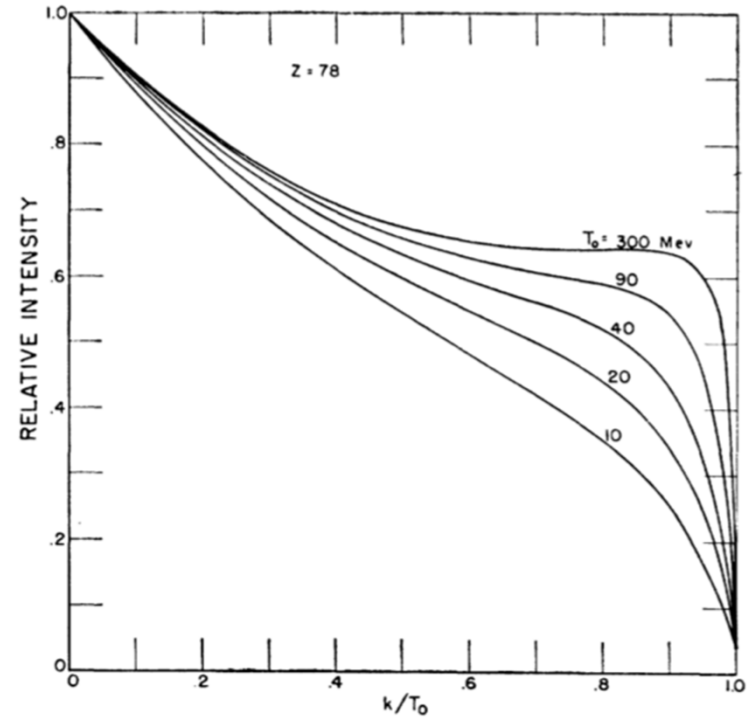


FIG. 4. Dependence of the bremsstrahlung spectrum shape on the electron kinetic energy for a platinum target ($Z=78$). The relative intensity (defined as proportional to the product of the photon energy and number per unit time) is integrated over the photon direction and is normalized to unity for zero photon energies. The intensity values were computed from Formula 3BS(e).

*Born-approximated Cross sections $d\sigma_k/dk$ w/ and w/o Coulomb correction
(from Koch and Motz)*

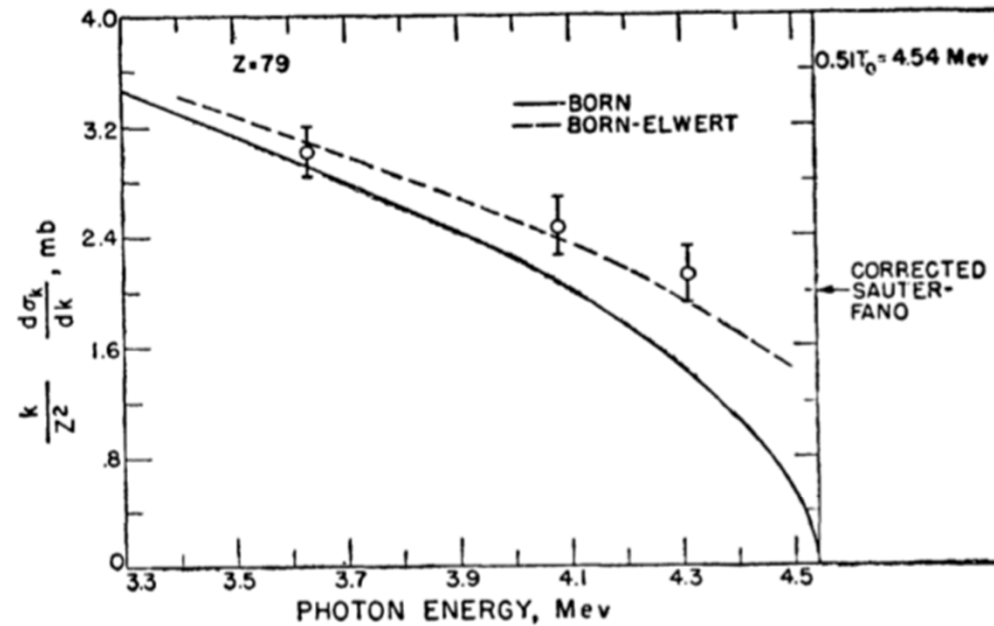


FIG. 21. Dependence of the bremsstrahlung cross section integrated over photon angle on the photon energy for 4.54-Mev electrons. The Born-approximation cross sections shown by the solid curve are calculated from Formula 3BN, and the Born-Elwert cross sections shown by the dashed curve are obtained from the product of Formula 3BN and the Elwert factor, Formula (II-4). The experimental values³⁶ are shown by the open circles for gold. The corrected Sauter-Fano values at the high-frequency limit are estimated in reference 21.

Total Bremsstrahlung cross section

✓ It can be rewritten as $\frac{d\sigma}{dk} = \left(1 + \frac{\eta}{Z}\right) \frac{d\sigma_n}{dk}$,

where η is the cross-section ratio $\eta = \frac{d\sigma_e}{dk} / \left(\frac{1}{Z^2} \frac{d\sigma_n}{dk}\right)$

Z²-dependency vs. Z-dependency

✓ Bremsstrahlung cross section for electron-electron interaction

– High-E approximation: Wheeler and Lamb formulae
(Phys Rev Vol 55, 858, 1939)

✓ Maximum photon energy in an electron-electron bremsstrahlung
(from Koch and Motz)

$$k_{\max} = F / (1 - \sqrt{F \cos \theta_0}), \quad \text{at the laboratory angle } \theta_0$$

where F is equal to $(E_0 - 1) / (E_0 + 1)$ and $0 \leq \theta_0 \leq \frac{\pi}{2}$.

Möller (Bhabha) Scattering

- ✓ Moller Scattering ($e^-e^- \rightarrow e^-e^-$)
- ✓ Bhabha scattering ($e^+e^- \rightarrow e^+e^-$)
- ✓ Moller and Bhabha scattering are collisions of incident electrons or positrons with atomic electrons.
- ✓ It is conventional to assume that these atomic electrons are “free” ignoring their atomic binding energy.
- ✓ The electrons in the e^-e^+ pair can annihilate and be recreated, contributing an extra interaction channel to the cross section.

$$\frac{Q_{max}}{E_{in}} = \frac{E_{in} - E_{out,min}}{E_{in}} = \frac{4mM}{(m+M)^2}$$

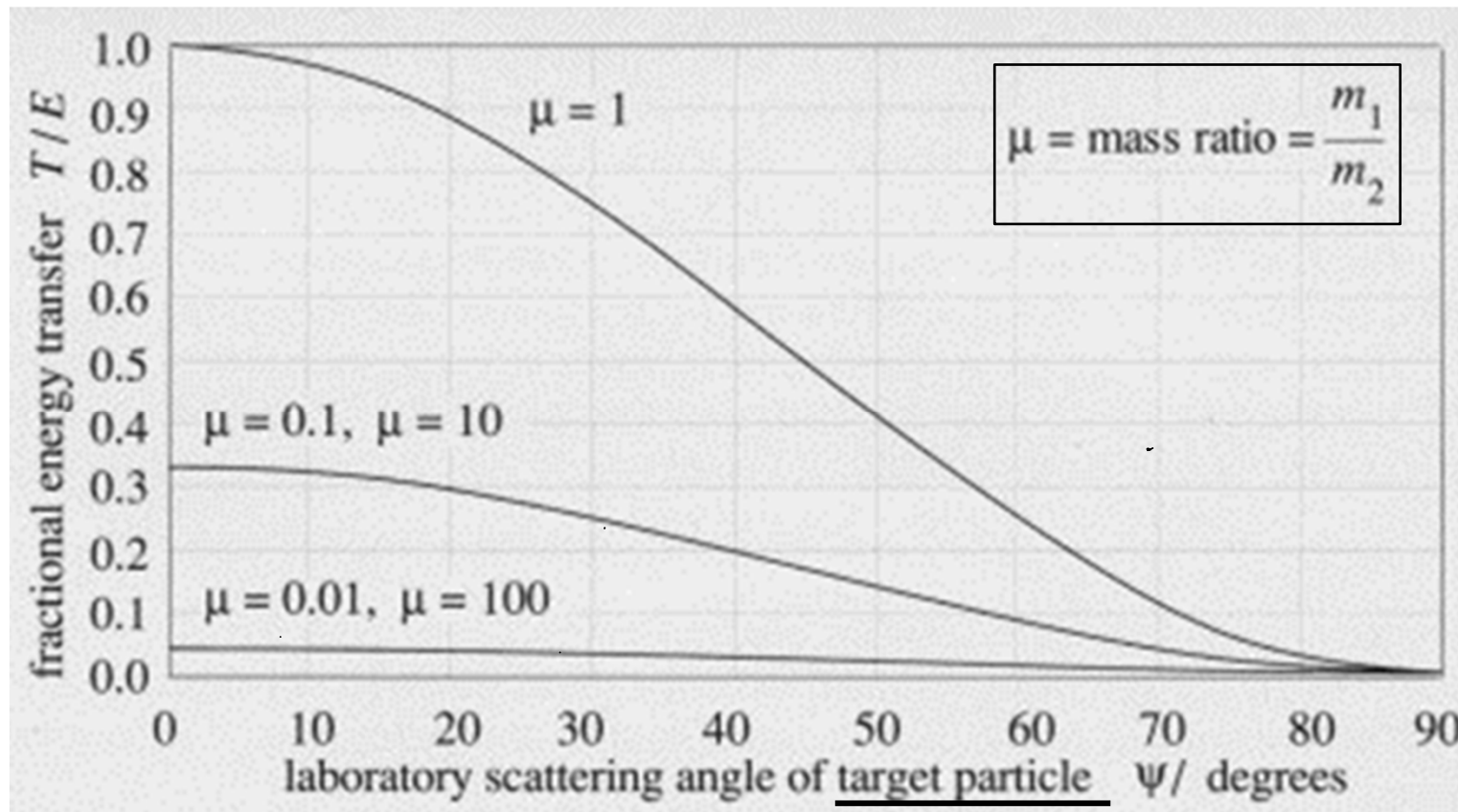


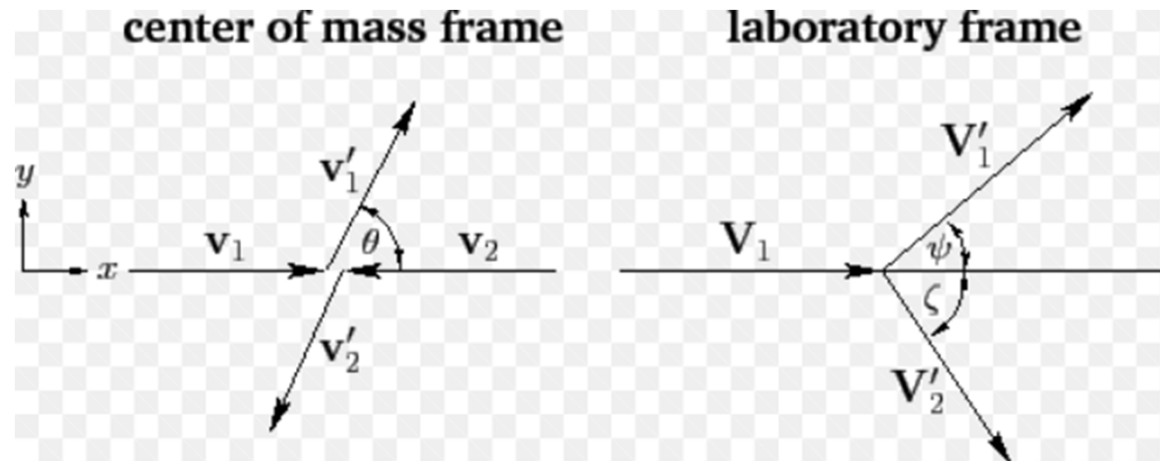
Figure 2-12 Energy transfer in elastic collisions. Fraction T/E of energy transferred from the projectile to the target in an elastic collision as function of the laboratory scattering angle ψ of the target. The fraction of transferred energy is symmetric with respect to a mass exchange $m_1 \rightarrow m_2, m_2 \rightarrow m_1$, it has a maximum for equal masses, $m_1 = m_2$, and it decreases with increasing scattering angle ψ .

Moller (Bhabha) Scattering (cont.)

- ✓ In the e^-e^- case, the “primary” electron can only give at most half its energy to the target electron if we adopt the convention that the higher energy electron is always denoted “the primary”. This is because the two electrons are indistinguishable. In the e^+e^- case, the positron can give up all its energy to the atomic electron.
- ✓ Moller and Bhabha cross sections scale with Z for different media. The cross section scales approximately as $1/v^2$, where v is the velocity of the scattered electron.
- ✓ Many more low energy secondary particles are produced from the Moller interaction than from the bremsstrahlung interaction.

➤ Bhabha scattering ($e^+e^- \rightarrow e^+e^-$)

- elastic positron-electron scattering where outgoing particles are distinguishable.

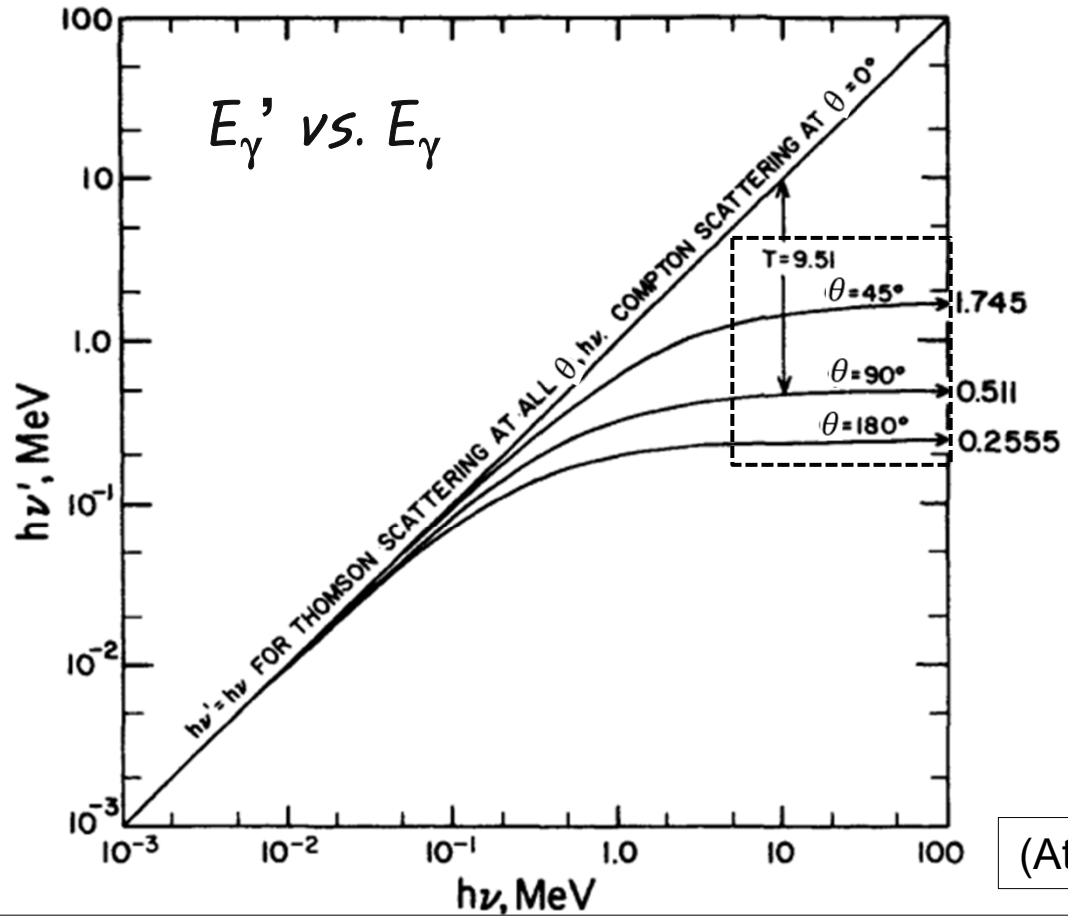


- Bhabha's theoretical formula (1935)

$$\left[\frac{d\sigma}{d\Omega} = \frac{e^4}{32\pi^2 \underline{E_{cm}^2}} \left[\frac{1 + \cos^4 \frac{\theta}{2}}{\sin^4 \frac{\theta}{2}} - \frac{2 \cos^4 \frac{\theta}{2}}{\sin^2 \frac{\theta}{2}} + \frac{1 + \cos^2 \theta}{2} \right] \right]$$

where θ is the scattering angle of electron in COM

Compton scattering



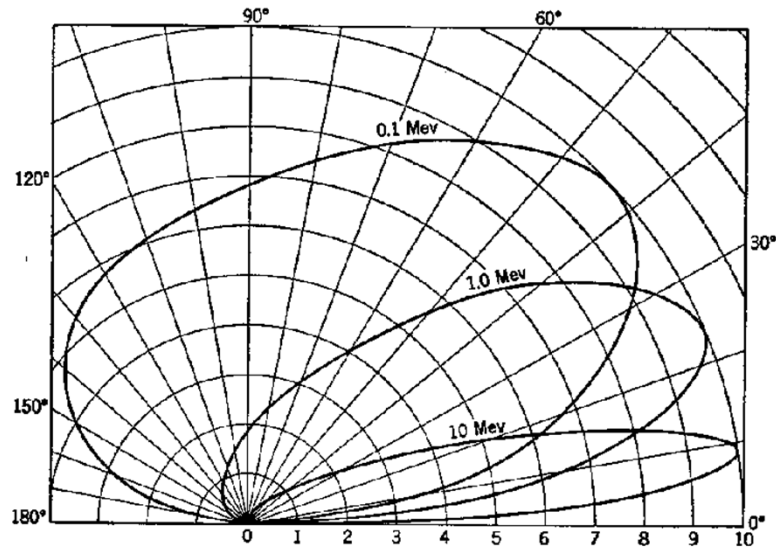
(Attix Fig 7.3)

$$\frac{h\nu'}{h\nu} = \frac{1}{1 + (h\nu/m_0c^2)(1 - \cos\theta)}$$

Thomson scattering
~ 1, at $h\nu \ll m_e c^2$ for all θ .

$$\frac{h\nu'}{h\nu} \approx \frac{m_0c^2}{h\nu(1 - \cos\theta)}, \text{ at } h\nu \gg m_e c^2 \text{ for } \theta \neq 0. \text{ Compton scattering}$$

= 1, at all $h\nu$ for $\theta = 0$.



relative energy per unit interval of angle
(uploaded by Alice Miceli)

Compton scattering

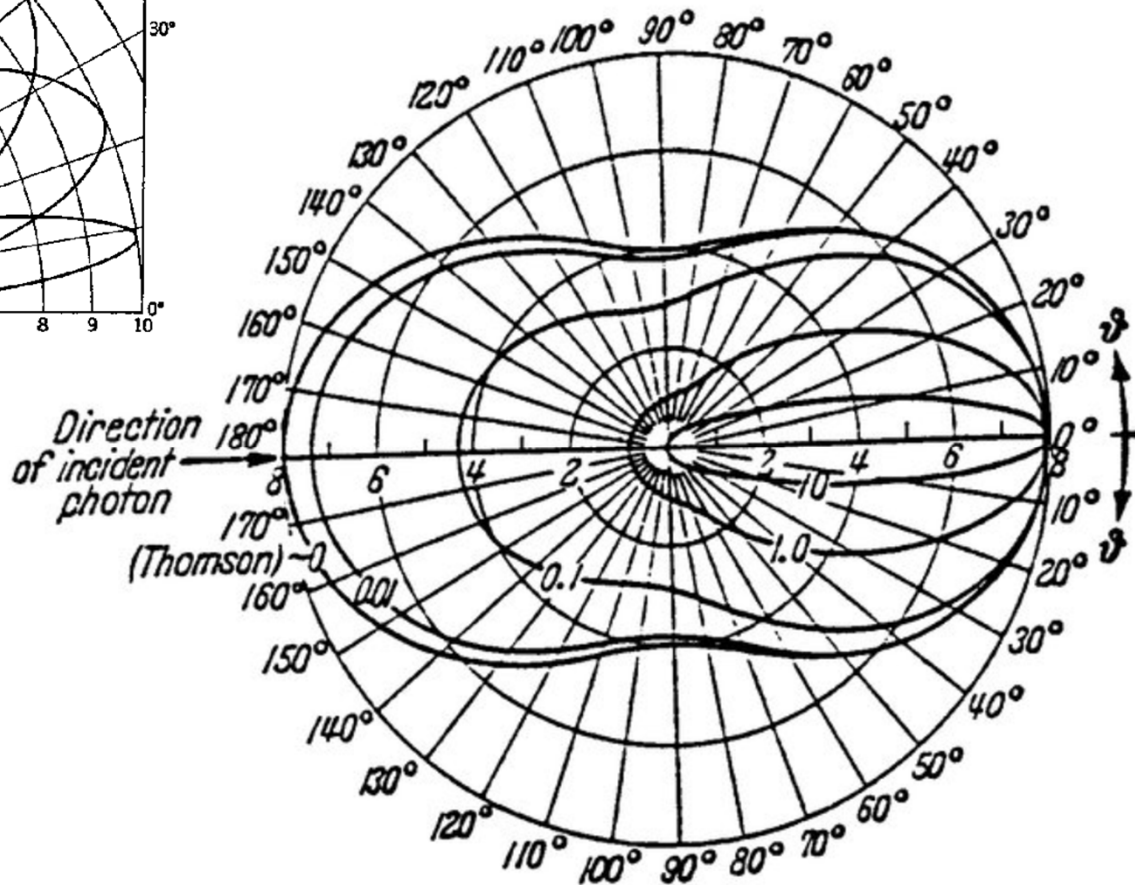
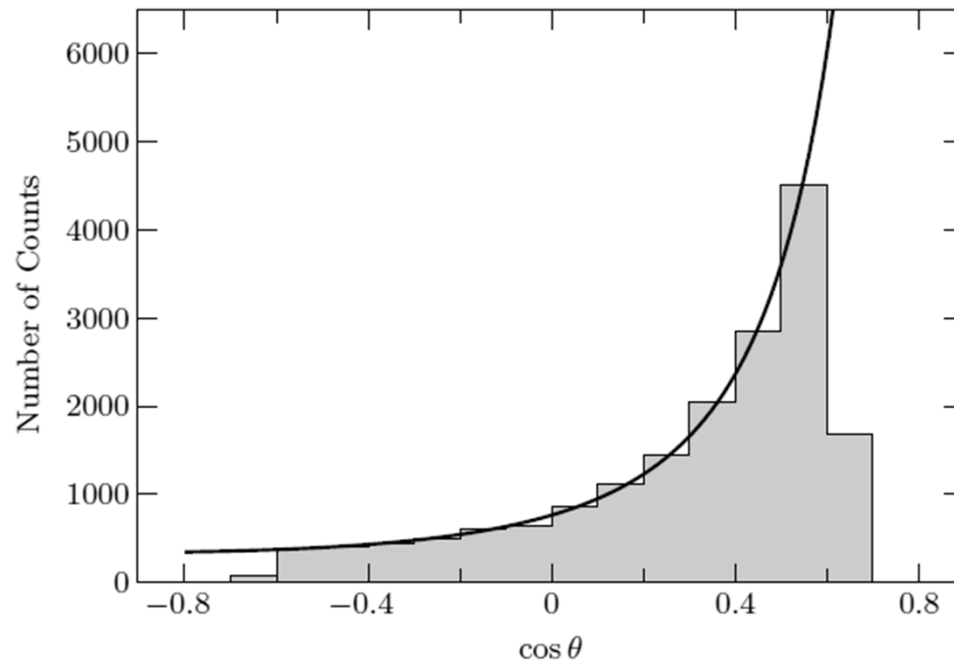


Figure 16. The number of scattered photons per unit solid angle, $d(\sigma_{\text{incoh}}) / d\Omega$, at scattering angle θ . Energies of the interacting photons are 0, 0.01, 0.1, 1.0 and 10 MeV. The radius of the polar diagram is given in units of 10^{-26} cm^2 per electron and steradian.

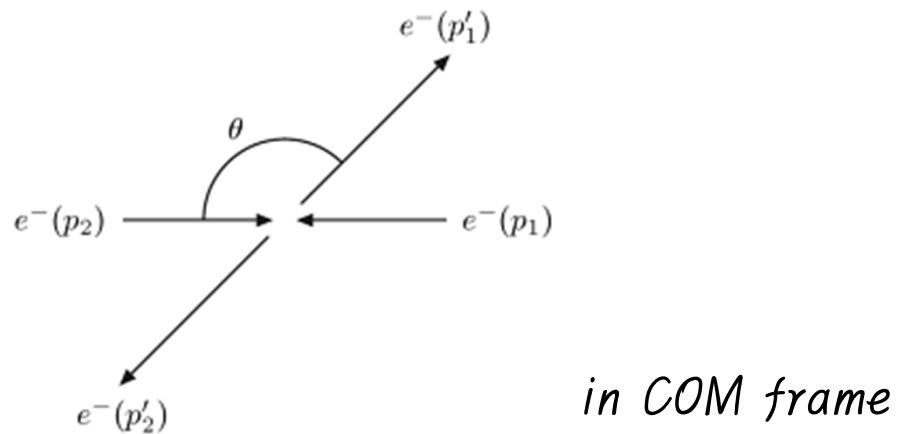
➤ Bhabha scattering ($e^+e^- \rightarrow e^+e^-$)

- Cross section in COM frame depends only on E and θ at E (GeV to TeV) $\gg m_e c^2$ (MeV).



*measurement taken at Stanford's SPEAR collider (early 1970s):
The number of events (and hence the differential cross section) increases as θ decreases, and goes to infinity in the limit $\theta \rightarrow 0$.*

- Moller scattering ($e^-e^- \rightarrow e^-e^-$)
 - elastic electron-electron scattering



$$\boxed{\frac{d\sigma}{d\Omega}} = \frac{d\sigma}{d\Omega}(\theta) = \frac{d\sigma}{d\Omega}(-\theta) = \frac{d\sigma}{d\Omega}(\pi - \theta)$$

because the outgoing particles are indistinguishable.

Positron Annihilation

- ✓ Two-photon “in-flight” annihilation ($e^+e^- \rightarrow 2\gamma$) can be modeled using the cross-section formulae of Heitler.

$$\boxed{\sigma(Z, E)} = \frac{Z\pi r_0^2}{\gamma + 1} \left[\frac{\gamma^2 + 4\gamma + 1}{\gamma^2 - 1} \ln \left(\gamma + \sqrt{\gamma^2 - 1} \right) - \frac{\gamma + 3}{\sqrt{\gamma^2 - 1}} \right]$$

E = total energy of the incident positron

γ = $E/m_e c^2$

r_0 = classical electron radius

- ✓ It is conventional to consider the atomic electrons to be free, ignoring binding effects.
- ✓ Three and higher-photon annihilations ($e^+e^- \rightarrow n\gamma$ [$n > 2$]) as well as one-photon annihilation, which is possible in the Coulomb field of a nucleus ($e^+e^-N \rightarrow \gamma N^*$), can be ignored as well.

Positron Annihilation (cont.)

- ✓ The higher-order processes are very much suppressed relative to the two-body process (by at least a factor of 1/137) while the one-body process competes with the two-photon process only at very high energies where the cross section becomes very small.

back-to-back annihilation by a positron at rest
vs. one-photon annihilation by a positron at high energy

- ✓ If a positron survives until it reaches the transport cut-off energy, it can be converted into two photons (annihilation at rest).

PHYSICAL REVIEW D

PARTICLES AND FIELDS

THIRD SERIES, VOLUME 35, NUMBER 1

1 JANUARY 1987

Tests of quantum electrodynamics with two-, three-, and four-photon final states from e^+e^- annihilation at $\sqrt{s} = 29$ GeV

E. Fernandez,* W. T. Ford, N. Qi, A. L. Read, Jr., and J. G. Smith
Department of Physics, University of Colorado, Boulder, Colorado 80309

T. Camporesi,† I. Peruzzi, and M. Piccolo
Istituto Nazionale di Fisica Nucleare, Laboratori Nazionali di Frascati, Frascati, Italy

H. T. Blume, R. B. Hurst, K. H. Lau, J. Pyrlík, J. P. Venuti, H. B. Wald, and Roy Weinstein
Department of Physics, University of Houston, Houston, Texas 77004

H. R. Band, M. W. Gettner, G. P. Goderre, J. H. Moromisato, W. D. Shambroom,‡
J. C. Sleeman, and E. von Goeler
Department of Physics, Northeastern University, Boston, Massachusetts 02115

W. W. Ash, G. B. Chadwick, R. E. Leedy, R. L. Messner, L. J. Moss, F. Müller,§
H. N. Nelson, D. M. Ritson, L. J. Rosenberg, D. E. Wisner, and R. W. Zdarko
Department of Physics and Stanford Linear Accelerator Center, Stanford University, Stanford, California 94305

D. E. Groom and P. G. Verdini
Department of Physics, University of Utah, Salt Lake City, Utah 84112

M. C. Delfino, B. K. Heltsley,** J. R. Johnson, T. L. Lavine, T. Maruyama, and R. Prepost
Department of Physics, University of Wisconsin, Madison, Wisconsin 53706

(Received 23 June 1986)

High-precision measurements of electron-positron annihilation into final states of two, three, and four photons are presented. The data were obtained with the MAC detector at the PEP storage ring of the Stanford Linear Accelerator Center, at a center-of-mass energy of 29 GeV. The measured $e^+e^- \rightarrow \gamma\gamma$ differential cross section is used to test the validity of quantum electrodynamics (QED) in this energy range; it agrees well with QED, and the limit on cutoff parameters for the electron propagator is $\Lambda > 66$ GeV. The measurement of $e^+e^- \rightarrow \gamma\gamma\gamma$ is used to test the QED calculations of order α^3 and to search for anomalies that would indicate the existence of new particles; the agreement with QED is excellent and no anomalies are found. Two events from the reaction $e^+e^- \rightarrow \gamma\gamma\gamma\gamma$ are found, in agreement with the QED prediction.

Range in water: positron vs. electron

TABLE I: SIMULATED AND EXPERIMENTAL POSITRON RANGE IN WATER.

$\beta_{max}(keV)$		Mean range	Max. range	Mean range	Max range
		PeneloPET (mm)	PeneloPET (mm)	[17] (mm)	[17] (mm)
635	¹⁸ F	0.61	2.3	0.64	2.3
960	¹¹ C	1.04	3.9	1.03	3.9
1,190	¹³ N	1.31	5.1	1.32	5.1
1,720	¹⁵ O	2.00	7.9	2.01	8.0
1,899	⁶⁸ Ga	2.21	8.9	2.24	8.9
3,400	⁸² Rb	4.24	16.7	4.29	16.5

source: Cal-Gonzalez et al., "Positron range effects in high resolution 3D PET imaging"

E(keV)	Electron range (mm)
1	68.3 x 10 ⁻⁶
10	2.64 x 10 ⁻³
100	0.143
500	1.76
1,000	4.43
2,000	9.85